Activities in $CaO-SiO_2-Al_2O_3$ Slags and Deoxidation Equilibria of Si and Al

HIROKI OHTA and HIDEAKI SUITO

By using the data in previous and present slag-metal equilibrium experiments, the activities of SiO_2 along the liquidus lines in $CaO-SiO_2-Al_2O_3$ slags were determined at 1823 and 1873 K from the reaction $\underline{Si} + 2\underline{O} = SiO_2$ (s), in which the oxygen activities were estimated from the measured oxygen contents or from the combination of nitrogen distribution ratios (L_N) and nitride capacities (C_N). The activities of Al_2O_3 were also determined from the reaction $2\underline{Al} + 3\underline{O} = Al_2O_3$ (s), in which the oxygen activities were estimated from the values for L_N and C_N, or from the reaction $3SiO_2$ (s) + $4\underline{Al} = 2Al_2O_3$ (s) + $3\underline{Si}$, in which the activities of SiO_2 and the contents of Al and Si along with the respective interaction coefficients were used. The activities of Al_2O_3 and CaO in the entire liquid region were estimated from the Rein and Chipman's activities of SiO_2 by using the method of Schuhmann. On the basis of these activities, the deoxidation equilibria of Si and Al in steels were discussed.

I. INTRODUCTION

IN ladle refining processes, the $CaO-SiO_2-Al_2O_3$ based slags with high CaO/SiO_2 ratio are commonly used for the production of high-quality steels. In the production of clean steels such as a tire cord steel,[1] these slags with low CaO/SiO_2 ratio are also used for the control of the inclusions composition after Si-Mn deoxidation processes. Thermodynamic analysis for the refining reactions in these processes requires a precise knowledge of the activities of Al_2O_3 and SiO_2 over a wide range of liquid composition.

Rein and Chipman[2] determined the activities of SiO_2 in the entire liquid region of the $CaO-SiO_2-Al_2O_3$ system at 1823 and 1873 K from the measurements of the silicon distribution between slags and Fe-Si-C alloys saturated with either graphite or silicon carbide under $P_{co} = 1$ atmosphere. On the basis of these activities of SiO_2, they calculated the activities of $AlO_{1.5}$ and CaO using the method of Schuhmann.[3] In this calculation, the activities in the $CaO-AlO_{1.5}$ binary system were taken as the starting points with the aid of the known free energies of the interoxide compounds and the accepted phase diagram. However, the activities of $AlO_{1.5}$ and CaO in the SiO_2-rich region are not reported, and in addition, the activities of $AlO_{1.5}$ calculated at 1873 K are given only at limited slag compositions.

Kay and Taylor[4] obtained the activities of SiO_2 at 1723, 1773, and 1823 K in the entire liquid region of this system by measurements of the equilibrium CO pressure in the reaction $SiO_2 + 3C = SiC + 2CO$, and the values at 1873 K were also estimated by extrapolation. The activities of Al_2O_3 and CaO at 1823 K calculated by the method of Schuhmann are reported in the entire liquid region. Ozturk and Fruehan[5] determined the isoactivity lines for SiO_2 at 1798 and 1873 K at low SiO_2 concentrations by using the method of Rein and Chipman.[2] The activities of CaO at limited slag compositions at 1873 K were determined from the measurements of sulfide capacity by Kalyanram *et al.*[6] It can be summarized from these previous results that the activities of SiO_2 obtained by Rein and Chipman[2] and Kay and Taylor[4] agree fairly well with each other, whereas those of Al_2O_3 and CaO are inconsistent to a significant degree.

In a series of our previous slag-metal equilibrium experiments[7–10] at 1823 and 1873 K, the activities of SiO_2 in the $CaO-SiO_2-Al_2O_3$ slags were determined from the reaction $\underline{Si} + 2\underline{O} = SiO_2$ (s), in which the activities of oxygen were estimated from the values for the nitrogen distribution ratio (L_N), coupled with those for the nitride capacity (C_N) obtained in independent gas-slag equilibrium experiments.[11] As a result, the activities of SiO_2 were found to be in satisfactory agreement with those by Rein and Chipman[2] and Kay and Taylor.[4] The reasons that the measured oxygen contents were not used for the estimation of oxygen activities were due to the large uncertainty resulting from the errors in oxygen analysis as well as those in the estimation of the activity coefficient of oxygen which was strongly influenced by even a small content of Ca.

The activities of Al_2O_3 were estimated from the exchange reaction $3SiO_2$ (s) + $4\underline{Al} = 2Al_2O_3$ (s) + $3\underline{Si}$, by using the activities of SiO_2, the contents of Al and Si, and the respective interaction coefficients for Al ($f_{\underline{Al}}$) and Si ($f_{\underline{Si}}$). As a result, the activities of Al_2O_3 along the compositions saturated with an Al_2O_3 and CaO crucibles were found to be significantly different from those by Rein and Chipman[2] and Kay and Taylor.[4]

In our recent studies, the first- and second-order interaction coefficients between Ca and O[12] were experimentally determined and the degree of supersaturation in alumina precipitation[13] was extensively studied as a function of slag composition in this system. By taking account of these results, the activities of SiO_2 in the $CaO-SiO_2-Al_2O_3$ slags at 1823 and 1873 K were determined from the reaction $\underline{Si} + 2\underline{O} = SiO_2$ (s), by using the analyzed silicon and oxygen contents obtained in previous[7–10,14] and the present additional equilibrium experiments. These results were compared with those estimated from the values for L_N and C_N. The activities of Al_2O_3 and CaO in the entire liquid

HIROKI OHTA, Research Associate, and HIDEAKI SUITO, Professor, are with the Institute for Advanced Materials Processing, Tohoku University, Sendai 980, Japan.

Manuscript submitted January 2, 1996.

Table I. Chemical Compositions of Metal and Slag Phases

[Al]		Metal			Slag				
Sol.	Insol.	[Si]	[Mn]	[O]	(CaO)	(SiO_2)	(Al_2O_3)	(MnO)	(Fe_tO)
(Mass ppm)		(Mass Pct)		(Mass ppm)	(Mass Pct)				
				1823 K					
CAS-12									
39.6	1.4	1.13	0.302	6.0	51.8	29.5	18.3	0.123	0.562
46.7	0.5	1.49	0.448	5.1	50.3	30.3	17.7	0.165	0.499
71.9	0.1	2.22	0.423	5.7	49.4	29.7	19.2	0.090	0.260
CAS-13									
24.3	0.3	1.06	0.290	5.2	48.8	34.2	15.3	0.314	0.304
29.9	0.5	1.56	0.451	7.4	51.2	35.9	11.0	0.318	0.599
35.0	0.7	2.13	0.390	7.3	49.6	35.9	12.2	0.221	0.311
				1873 K					
ACS-7									
5.7	2.0	1.80	0.0210	26.7	15.0	49.0	34.0	0.413	1.17
20.4	1.1	2.30	0.0051	27.7	13.4	49.9	34.7	0.080	1.21
31.7	1.4	3.11	0.0327	25.4	12.9	49.2	35.4	0.475	1.36

region were estimated from the Rein and Chipman's activities for SiO_2,[2] by using the method of Schuhmann coupled with the corresponding activities along the liquidus lines. On the basis of these activities, the deoxidation equilibria of Si and Al were discussed by taking the examples of a tire cord and low carbon sheet steels.

II. ESTIMATION OF ACTIVITIES

The slag and metal compositions obtained in the present work are given in Table I. Detailed descriptions of the experimental method and chemical analyses are already given in previous reports.[7,8,10,14] The present and previous slag compositions at 1823 and 1873 K are shown by half-filled and open circles in Figures 1(a) and (b), respectively. Table II shows the symbols used in this work for previous and the present slag compositions. The open marks represent the results for the activities of SiO_2 calculated from the analyzed silicon and oxygen contents and those for the activities of Al_2O_3 determined from the reaction: $4\underline{Al} + 3SiO_2$ (s) $= 2Al_2O_3$ (s) $+ 3\underline{Si}$ using the analyzed contents of Si and Al. The half-filled marks represent the results calculated from the values for L_N and C_N. Details of these two methods will be described in Sections A through C. The interaction coefficients used in this study are summarized in Table III. In the case of the interaction coefficients whose temperature dependence was not reported, the values at 1823 K were estimated from those at 1873 K by assuming a regular solution.

A. *Activity of SiO_2*

Isoactivity lines for SiO_2 at 1823 and 1873 K reported by Rein and Chipman[2] and Kay and Taylor[4] are replotted in Figures 2(a) and (b), respectively, in which the lines by Kay and Taylor at 1873 K correspond to those obtained by extrapolation. The liquidus lines are drawn based on the accepted phase diagram;[20] the lines were assessed in a previous study.[21] By using the data of Tamura and Suito,[7] Cho and Suito,[9] and Inoue and Suito,[8] the activities of SiO_2 were obtained from Eq. [1]; the activities were derived from the nitrogen distribution ratio, L_N {=(mass pct N)/[mass pct N]}, and the nitride capacity, C_N {=(mass pct N)$\cdot P_{O_2}^{3/4}/P_{N_2}^{1/2}$}, coupled with the activities of oxygen in the reaction $\underline{Si} + 2\underline{O} = SiO_2$ (s) ($\Delta G^0_{Si} = -581{,}900 + 221.8T$ J/mol[15,22]).

$$\log a_{SiO_2} = 4/3 \log (C_N/L_N) + \log (K_{Si} \cdot K_O^2 \cdot f_{\underline{N}}^{4/3} \cdot a_{\underline{Si}}/K_N^{4/3}) \quad [1]$$

where K_N is the equilibrium constant for the reaction $1/2N_2 = \underline{N}$ ($\Delta G^0_N = 3600 + 23.9T$ J/g·atm[15]); K_O is that for the reaction $1/2O_2 = \underline{O}$ ($\Delta G^0_O = -117{,}000 - 2.9T$ J/g·atm[15]); K_{Si} is that for the reaction $\underline{Si} + 2\underline{O} = SiO_2$ (s); and $f_{\underline{N}}$ and $a_{\underline{Si}}$ are the activity coefficient of N and the activity of Si referred to a dilute solution of 1 mass pct standard state, respectively.

These results at 1823 and 1873 K are indicated by half-filled marks in Figures 3 and 4, respectively, in which the range of the experimental scatter is shown by a vertical line. The values along the liquidus lines obtained by Rein and Chipman[2] and Kay and Taylor[4] shown in Figure 2 are also indicated by solid and dash-dotted lines, respectively.

The activities of SiO_2 were also evaluated from the reaction $\underline{Si} + 2\underline{O} = SiO_2$ (s), in which the activities of oxygen were derived from the analyzed oxygen contents. In the present study, the data in the equilibrium experiments by Tamura and Suito,[7] Cho and Suito,[9] and Inoue and Suito[8] at 1823 and 1873 K, those by Lee and Suito[10] and Ohta and Suito[14] at 1873 K, and the present results were used. These results are shown by open marks in Figures 3 and 4. It can be seen that the activities of SiO_2 determined by these two methods mentioned previously agree fairly well with each other and fall on the lines obtained by previous workers.[2,4,5] However, the activities of SiO_2 at $X_{SiO_2} = 0.1$ (CAS-7 at 1823 K and CAS-8 at 1873 K) estimated from the analyzed oxygen content are greater than those estimated from the L_N and C_N values due to the supersaturated oxygen.[13]

When the regular solution model is applied to the CaO-SiO_2-$AlO_{1.5}$ system, the activity coefficient of SiO_2 at a given $N_{AlO_{1.5}}/N_{CaO}$ ratio can be expressed as

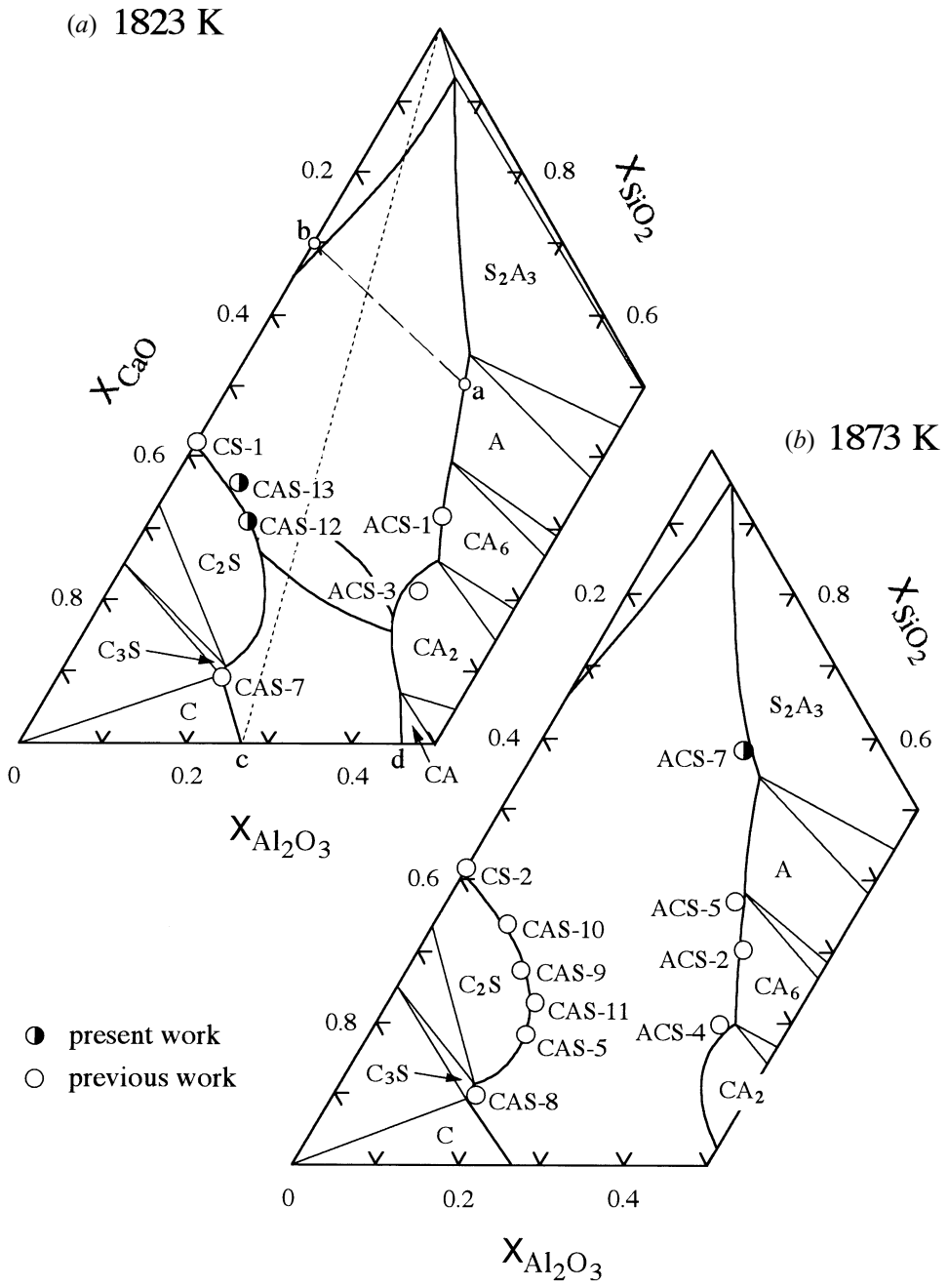

Fig. 1—Present and previous[7,8,10,14] experimental slag compositions at (*a*) 1823 K and (*b*) 1873 K.

$$R T \ln \gamma_{SiO_2} = \alpha \cdot N_{AlO_{1.5}}{}^2 + \beta \qquad [2]$$

where α and β are constants.

By using the isoactivity lines for SiO_2 by Rein and Chipman[2] shown in Figure 2, the relations given by Eq. [2] are plotted as a function of the $N_{AlO_{1.5}}/N_{CaO}$ ratio in Figure 5, in which the data by Ozturk and Fruehan[5] are also indicated by open marks. In order to obtain the activity coefficients of SiO_2 in an infinite dilute solution range of SiO_2 in the $CaO\text{-}AlO_{1.5}$ binary slags, the lines indicated by dotted lines in Figure 5 were extrapolated to the binary slag compositions. These values were taken as one of the starting points in the Gibbs–Duhem integration so that the activities of Al_2O_3 and CaO were calculated.

B. *Isoactivity Lines for Al_2O_3*

The activity coefficients of Al_2O_3 were calculated from the following Schuhmann method[3] based on the activity coefficients of SiO_2 derived from the SiO_2 activities by Rein and Chipman.[2]

$$\log \gamma^{II}_{Al_2O_3} = \log \gamma^{I}_{Al_2O_3} - \int_{\log \gamma^{I}_{SiO_2}}^{\log \gamma^{II}_{SiO_2}} \left(\frac{\delta n_{SiO_2}}{\delta n_{Al_2O_3}}\right)_{\gamma_{SiO_2},\, n_{CaO}} d \log \gamma_{SiO_2} \qquad [3]$$

where γ^{I}_{MO} and γ^{II}_{MO} are the activities of MO at initial and final states, respectively, and n_i is the number of moles of component i.

In the determination of $\gamma^{I}_{Al_2O_3}$ values in the liquid region

Table II. Symbols Used in This Work for the Present and Previous Experimental Data

Slag	This work	Tamura[7]	Inoue[8]	Cho[9]	Lee[10]	Ohta[14]
			1823 K			
ACS-1		□, ◨				
ACS-3		□, ◨				
CS-1			h , ▽			
CAS-13	q					
CAS-12	q					
CAS-7		□, ◨				
			1873 K			
ACS-7	q					
ACS-5					⬠	g
ACS-2		□, ◨		r , ◆	⬠	g
ACS-4		□, ◨		r , ◆	⬠	g
CS-2			h , ▽			g
CAS-10					⬠	g
CAS-9		□, ◨			⬠	g
CAS-11						g
CAS-5		□, ◨		r , ◆		g
CAS-8		□, ◨		r , ◆		g

on the right-hand side of the SiO_2 apex-point *c* join (Figure 1(a)), the $\gamma_{Al_2O_3}$ values along the Al_2O_3 saturation line and those[2] in the CaO-Al_2O_3 binary system (line *c–d* in Figure 1(a)) were used. In the determination of $\gamma^i_{Al_2O_3}$ values in the liquid region on the left-hand side of the SiO_2 apex-point *c* join, the following method was used, since the $\gamma_{Al_2O_3}$ values along the $2CaO{\cdot}SiO_2$, $3CaO{\cdot}SiO_2$, and CaO saturation lines could not be accurately determined in previous works, as will be described later. Point *a* in Figure 1(a) on the Al_2O_3 saturation line with the $X_{CaO}/X_{SiO_2} = 0.3/0.7$ was joined with the Al_2O_3 apex, and point *b* was obtained by extrapolation of this joined line to the CaO-SiO_2 binary system. The activity coefficients of Al_2O_3 on the line *a–b* were determined from Eq. [3]. By taking these values as the starting points, the $\gamma_{Al_2O_3}$ values in the liquid region on the left-hand side were determined. The isoactivity lines for Al_2O_3 at 1823 and 1873 K are shown in Figures 6 and 7, respectively, along with those reported by Rein and Chipman[2] and Kay and Taylor.[4] The present results are significantly different from those by previous workers, but with respect to the slag composition dependence, the present results show a similar trend to those by Kay and Taylor, as shown in Figure 6.

The activities of Al_2O_3 along the liquidus lines saturated with Al_2O_3 and CaO crucibles were calculated from the exchange reaction $4\underline{Al} + 3SiO_2\ (s) = 2Al_2O_3\ (s) + 3\underline{Si}$ ($\Delta G^0 = -658{,}300 + 107.2T$ J/mol[15,22]), by using the Rein and Chipman values[2] for the activities of SiO_2, the analyzed contents of Al and Si, and the respective interaction coefficients. The results at 1823 and 1873 K are shown by open marks with the range of the experimental scatter in Figures 8 and 9, respectively. The present results determined by the method of Schuhmann[3] and the previous values[2,4] are also shown by the different lines.

The activities of Al_2O_3 can be estimated from the values for C_N and L_N in a manner similar to Eq. [1] as

Table III. Interaction Coefficients Used in the Present Work[15]

i	*j*	e_i^j	r_i^j (r_i^{ij})	Ref.
Al	Al	$0.011 + 63/T$	$-0.0011 + 0.17/T$	
	C	0.091	−0.004	
	Ca	−0.047	——	16
	O	$11.95 - 34740/T$	——	
	Si	0.056	−0.0006	
	Ti	0.0040	——	17
Ca	Al	−0.072	0.0007	
	C	−0.34	0.012	
	Ca	−0.002	——	
	O	−9000	3.6×10^6 (2.9×10^6)*	12
		−2500	2.6×10^5 (2.1×10^5)**	
	Si	−0.097	0.0009	
	Mn	−0.0156	——	18
O	Al	$7.15 - 20600/T$	1.7	
	C	−0.45	——	
	Ca	−3600	5.7×10^5 (2.9×10^6)*	12
		−990	4.2×10^4 (2.1×10^5)**	
	O	$0.734 - 1750/T$	——	
	Si	−0.131	0	
	Ti	−0.6	0.031	
	Mn	−0.021	0	
Si	Al	0.058	——	
	C	$-0.023 + 380/T$	——	
	Ca	−0.067	——	16
	O	−0.23	——	
	Si	$0.089 + 34.5/T$	$-0.0055 + 6.5/T$	
	Ti	1.23	——	19
	Mn	0.002	——	
Mn	C	−0.07	——	
	Ca	−0.023	——	18
	O	−0.083	——	
	Si	0	0	
	Ti	−0.05	——	19
	Mn	0	0	

*[%Ca] + 2.51[%O] < 0.005
**[%Ca] + 2.51[%O] = 0.005 − 0.016

$$\log a_{Al_2O_3} = 2\log(C_N/L_N) + \log(K_{Al}\cdot K_O^3\cdot f_{\underline{N}}^2\cdot a_{\underline{Al}}^2/K_N^2) \quad [4]$$

where K_{Al} is the equilibrium constant for the reaction: $2\underline{Al} + 3\underline{O} = Al_2O_3\ (s)$ ($\Delta G^0_{Al} = -1{,}202{,}000 + 386.3T$ J/mol[15,22]).

The results from Eq. [4] are shown in Figures 8 and 9 by half-filled marks with the range of the experimental scatter. The data points determined by these two methods scatter to a considerable degree in comparison with the results for the activities of SiO_2 shown in Figures 3 and 4. This is supposed to be due to the large uncertainty resulting from the errors in the chemical analysis of Al content and those in the estimation of the SiO_2 activities, particularly, at the compositions with low SiO_2 contents.

C. *Isoactivity Lines for CaO*

The activity coefficients of CaO were estimated from the Schuhmann method based on those of SiO_2 in a manner sim-

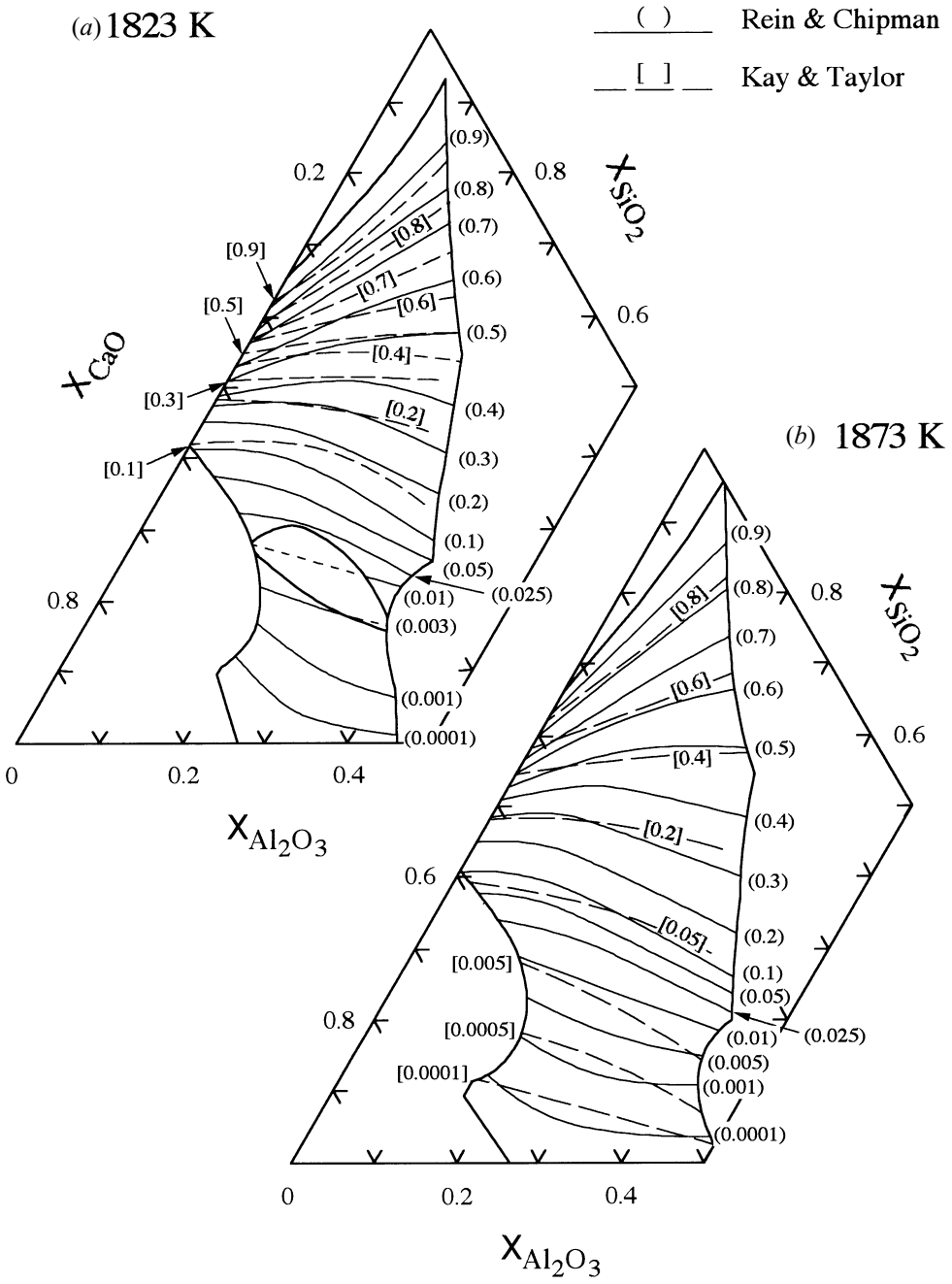

Fig. 2—Isoactivity lines for SiO_2 obtained by previous workers[2,4] at (*a*) 1823 K and (*b*) 1873 K.

ilar to the determination of the activity coefficients of Al_2O_3. In this calculation, the activities of CaO in $CaO\text{-}Al_2O_3$[2] and $CaO\text{-}SiO_2$[2] binary systems and those along the $2CaO{\cdot}SiO_2$ saturation line, which were obtained from the combination of the value of the free energy of its formation[23] and the activities of SiO_2, were taken as the starting points. The results at 1823 and 1873 K are shown in Figures 10 and 11, respectively, together with the results by Rein and Chipman[2] and Kay and Taylor.[4] It can be seen that the present results are in general accord with previous results.

III. DEOXIDATION EQUILIBRIA OF Si AND Al

On the basis of the activities in the $CaO\text{-}SiO_2\text{-}Al_2O_3$ slags estimated in this study, deoxidation equilibria of Si and Al are discussed by taking the examples of a tire cord steel and a Ti-containing low carbon sheet steel.

A. *Tire Cord Steel*

The contents of O and Al in tire cord steel (C = 0.8, Si = 0.3, and Mn = 0.6 in mass pct) were determined at 1823 K as a function of the inclusions composition in the $CaO\text{-}SiO_2\text{-}Al_2O_3$ system. The oxygen contents were calculated at [mass pct Si] = 0.3 from the equilibrium constant for the reaction $\underline{Si} + 2\underline{O} = SiO_2$ (s), the activities of SiO_2, and the respective interaction coefficients, by using the iterative method. The isoconcentration lines for oxygen (mass ppm) are shown by broken lines in Figure 12(a). Similarly, the isoconcentration lines for aluminum were obtained at [mass

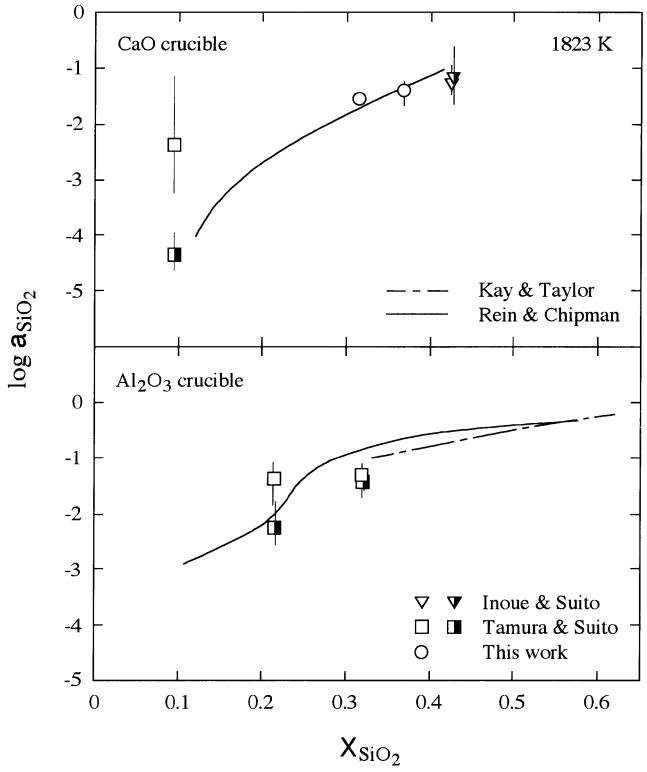

Fig. 3—Activities of SiO_2 along the liquidus lines saturated with CaO and Al_2O_3 crucibles at 1823 K.

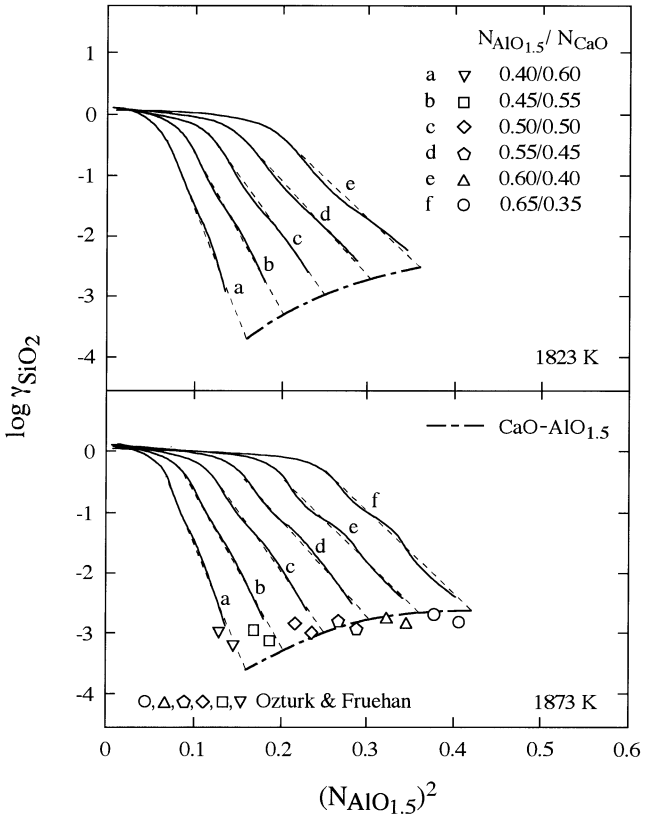

Fig. 5—Activity coefficients of SiO_2 in logarithmic form plotted against the second power of mole fraction of $AlO_{1.5}$ in the $CaO\text{-}SiO_2\text{-}AlO_{1.5}$ system.

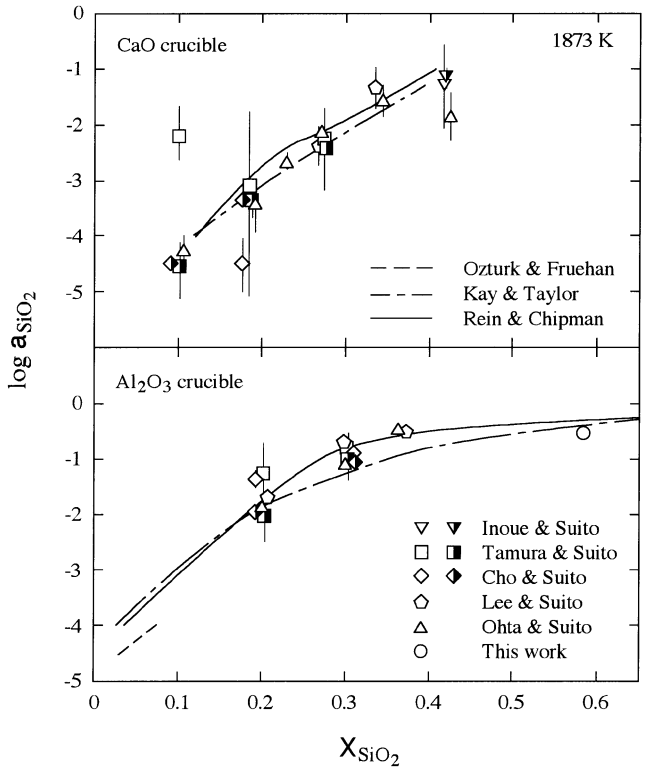

Fig. 4—Activities of SiO_2 along the liquidus lines saturated with CaO and Al_2O_3 crucibles at 1873 K.

pct Si] = 0.3 from the reaction $4\underline{Al} + 3SiO_2\ (s) = 2Al_2O_3\ (s) + 3\underline{Si}$, by using the activities of SiO_2 and Al_2O_3. The results (mass ppm) are shown in Figure 12(b) by broken lines. The MnO contents in the $CaO\text{-}SiO_2\text{-}Al_2O_3$ slags were also determined at [mass pct Mn] = 0.6 and [mass pct Si] = 0.3 from the reaction $\underline{Mn} + 1/2SiO_2\ (s) = MnO\ (s) + 1/2\underline{Si}$ ($\Delta G^0 = 2{,}800 + 17.4T$ J/mol[15,22,24]), using the activities of SiO_2 and the activity coefficients of MnO.[14] The results (mass pct) are plotted in the $CaO\text{-}SiO_2\text{-}Al_2O_3$ ternary system, as shown in Figure 12(b) by dash-dotted lines. The Fe_tO contents could not be determined in this study, since the activity coefficients of Fe_tO were not available in the SiO_2-rich region of this system. It should be noted that point *A* in Figure 12(a), which is the liquid composition at the ternary eutectic point (1438 K) in equilibrium with anorthite, pseudowollastonite, and tridymite, cannot be regarded as the $CaO\text{-}SiO_2\text{-}Al_2O_3$ ternary system under the present conditions because of high MnO content. It can be seen that the inclusions with the composition at point *A* are in equilibrium with the steels containing a considerably high level of oxygen (90 mass ppm) and an extremely low level of aluminum (0.5 mass ppm).

The inclusions with the liquid composition at the ternary eutectic point *B* (1539 K, pseudowollastonite, anorthite, and gehlenite) are in equilibrium with the oxygen content of 50 mass ppm and the aluminum content of 2 mass ppm. The MnO content in the inclusions at point B is relatively small, about 3 mass pct. It is important to realize that the control of Al level within a narrow range, which is markedly in-

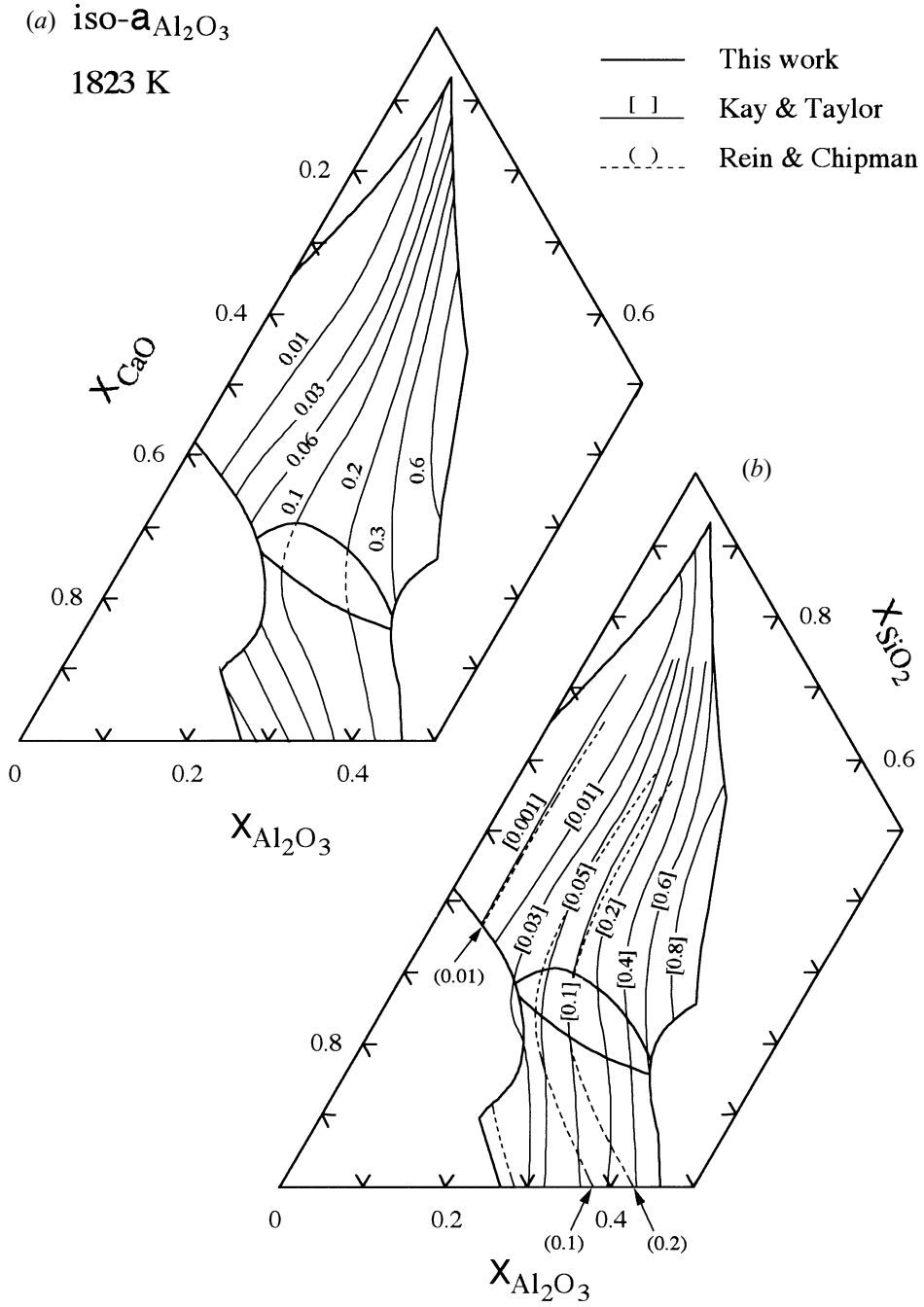

Fig. 6—Isoactivity lines for Al_2O_3 in the CaO-SiO_2-Al_2O_3 system at 1823 K obtained from (*a*) present and (*b*) previous[2,4] studies.

fluenced by the Al content in ferrosilicon alloys, is the key to the production of a tire cord steel containing deformable inclusions with a low melting point.

B. *Low Carbon Sheet Steel*

The Si contents in Ti-containing low carbon sheet steel (Al = 0.05, Mn = 0.15, and Ti = 0.05 in mass pct) in equilibrium with the top slags of the CaO-SiO_2-Al_2O_3 system were calculated at [mass pct Al] = 0.05 from the reaction $4\underline{Al} + 3SiO_2\ (s) = 2Al_2O_3\ (s) + 3\underline{Si}$. The isoconcentration lines for Si (mass pct) at 1823 K are shown in Figure 13(a), indicating that the Si contents increase with an increase in the SiO_2 content. The contents of O and Ca calculated from the reaction $2\underline{Al} + 3\underline{O} = Al_2O_3\ (s)$ and $2/3\underline{Al} + CaO\ (s) = 1/3Al_2O_3\ (s) + \underline{Ca}$ ($\Delta G^0 = 244{,}000 - 19.9T$ J/mol[12,15,22,25]), respectively, are shown in Figures 13(b) and 14(a). When the top slag composition is chosen as point *P* with $X_{SiO_2} = 0.1$ and $X_{CaO}/X_{Al_2O_3} = 2.5$, the equilibrium contents of Si, O, and Ca are determined as 0.7 mass pct, 1 mass ppm, and 3 mass ppm, respectively.

In the production of low carbon sheet steels, the CaO-SiO_2-Al_2O_3 top slag with the composition of point *P*, which contains about 10 mass pct MgO, is widely used in ladle refining processes. It is reported that the total oxygen content is approximately in the range of 10 to 30 mass ppm,

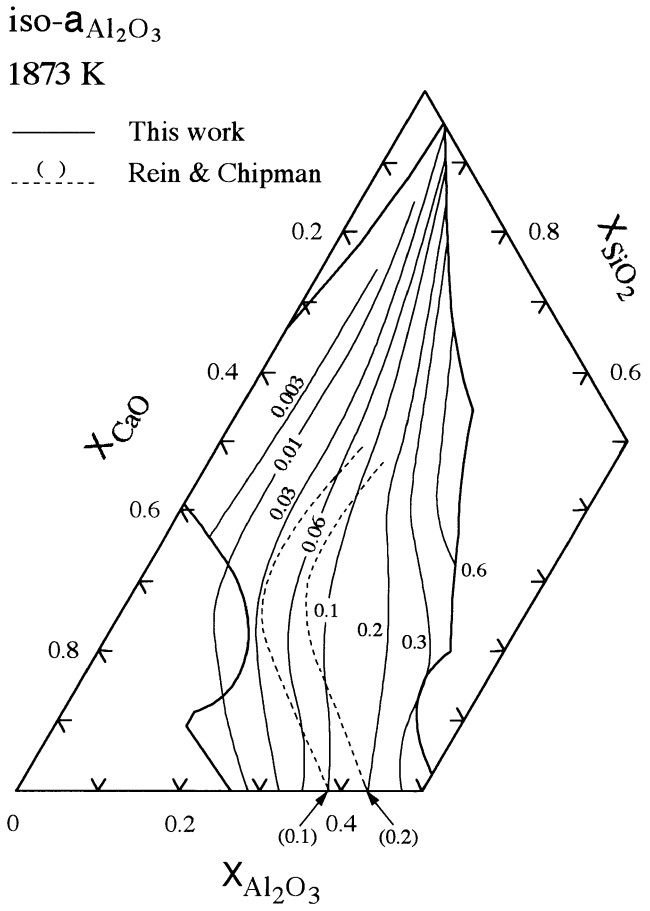

Fig. 7—Isoactivity lines for Al_2O_3 in the $CaO-SiO_2-Al_2O_3$ system at 1873 K.

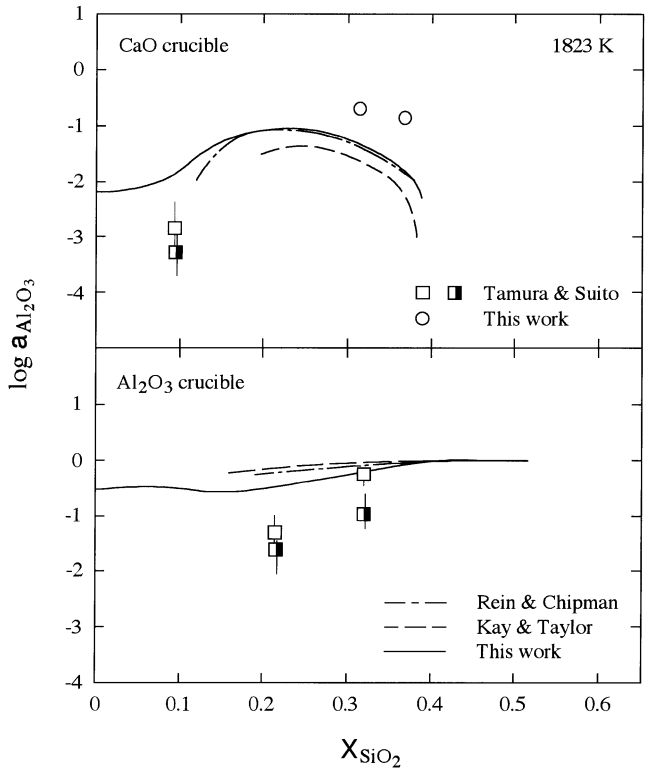

Fig. 8—Activities of Al_2O_3 along the liquidus lines saturated with CaO and Al_2O_3 crucibles at 1823 K.

which is considerably higher than the equilibrium value. If the total oxygen observed in practice is regarded as a dissolved oxygen, the top slag compositions in equilibrium with 10 to 30 mass ppm oxygen are those represented by the shaded area shown in Figure 13(b). However, the Si levels in equilibrium with these top slags are above 7 mass pct, which is considerably higher than the observed values, such as below about 0.1 mass pct. This discrepancy between the calculated and observed values with respect to Si and O is supposed to be due to considerably higher Fe_tO contents observed in practical top slags compared with the equilibrium value.

The Fe_tO contents in the $CaO-SiO_2-Al_2O_3$ slags were calculated at [mass pct Al] = 0.05 from the reaction $3Fe\ (l) + Al_2O_3\ (s) = 3Fe_tO\ (l) + 2\underline{Al}$ ($\Delta G^0 = 853{,}900 - 239.9T$ J/mol[15,22,26]), using the activity coefficients of Fe_tO.[10] The isoconcentration lines for Fe_tO (mass pct) are shown in Figure 14(b). It can be seen that the equilibrium content of Fe_tO at point P is much less than the observed value, such as about 1 mass pct, thus leading to the decrease in the Si content and the increase in the O content to a considerable degree. In the case that most of the total oxygen is regarded as the suspended Al_2O_3, most of the dissolved O content in practice is considered to correspond to the value determined by the $\underline{Al}/(Al_2O_3)$ equilibrium rather than that by the $Fe/(Fe_tO)$ equilibrium.

The values of Ca level in the production of low carbon

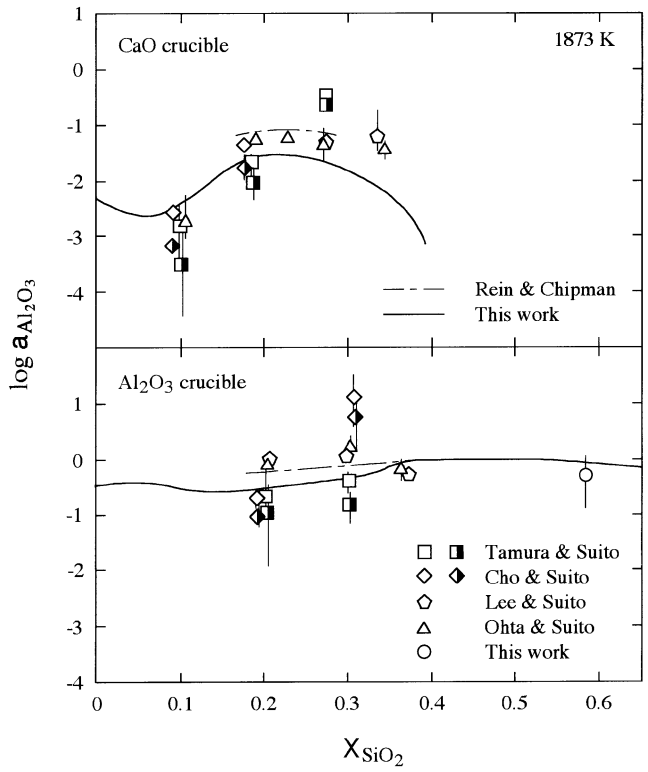

Fig. 9—Activities of Al_2O_3 along the liquidus lines saturated with CaO and Al_2O_3 crucibles at 1873 K.

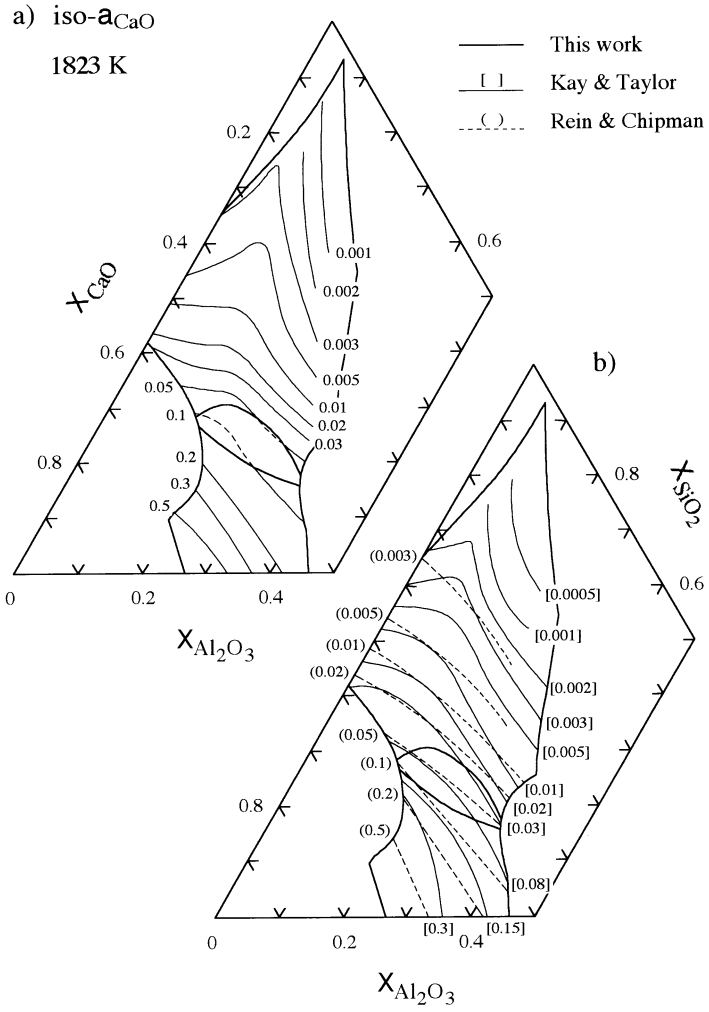

Fig. 10—Isoactivity lines for CaO in the $CaO-SiO_2-Al_2O_3$ system at 1823 K obtained from (*a*) present and (*b*) previous[2,4] studies.

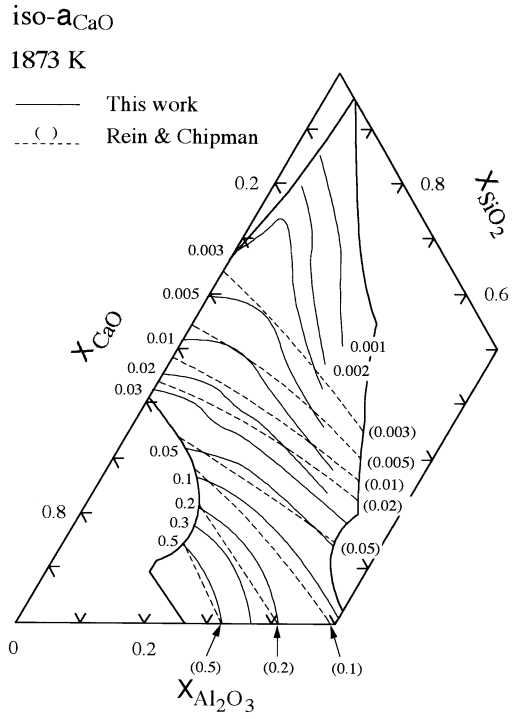

Fig. 11—Isoactivity lines for CaO in the $CaO-SiO_2-Al_2O_3$ system at 1873 K.

sheet steels are not reported, because the Ca treatment is not usually carried out. The Ca contents in high carbon steels after the Ca treatment, which are reported in the range of 20 to 30 mass ppm, are significantly greater than the equilibrium value. The Ca level in Figure 14(a) is different because of the difference in solute contents. This discrepancy also suggests that most of the observed total Ca corresponds to the suspended Ca-containing inclusions.

IV. CONCLUSIONS

The activities of SiO_2 over the entire liquid region in the $CaO-SiO_2-Al_2O_3$ system, which were determined by Rein and Chipman[2] and Kay and Taylor[4] using different experimental methods, were confirmed to be consistent with the present results on the liquidus lines obtained by a slag-metal equilibration technique. It was found, however, that although the activities of Al_2O_3 on the liquidus lines determined in slag-metal equilibrium experiments scattered to a considerable degree, these values agreed roughly with those determined by the Schuhmann method based on the SiO_2 activities within the limit of experimental uncertainty. To improve the accuracy in the activities of Al_2O_3 over entire liquid region, these values on the $2CaO{\cdot}SiO_2$ saturation line,

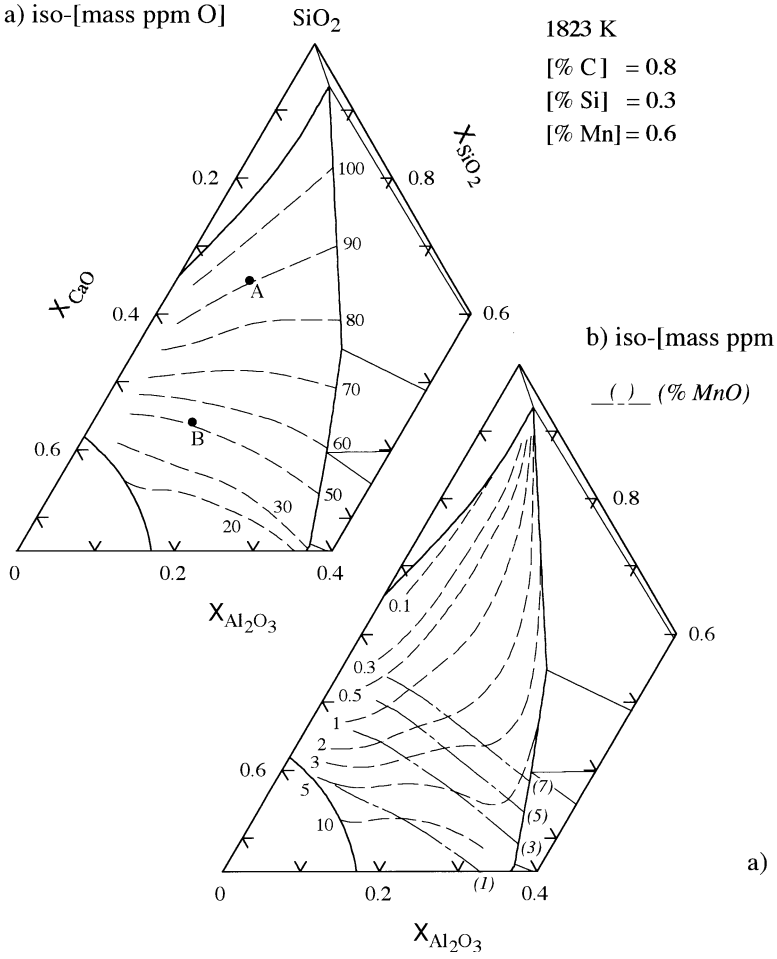

Fig. 12—(*a*) Iso-[mass ppm O] and (*b*) iso-[mass ppm Al] lines at 1823 K for tire cord steel.

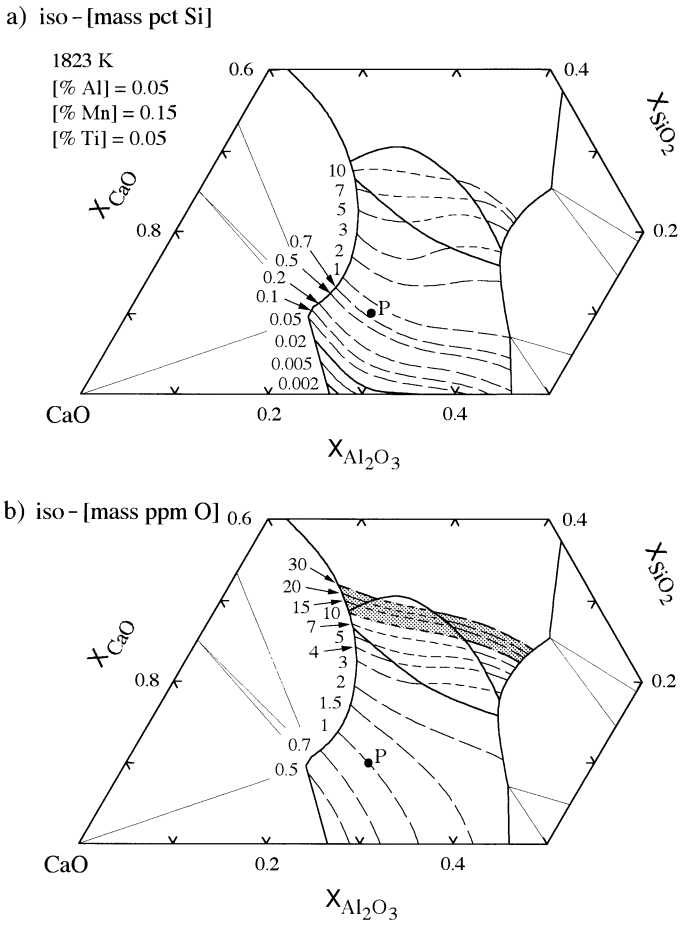

Fig. 13—(*a*) Iso-[mass pct Si] and (*b*) iso-[mass ppm O] lines at 1823 K for low carbon sheet steel.

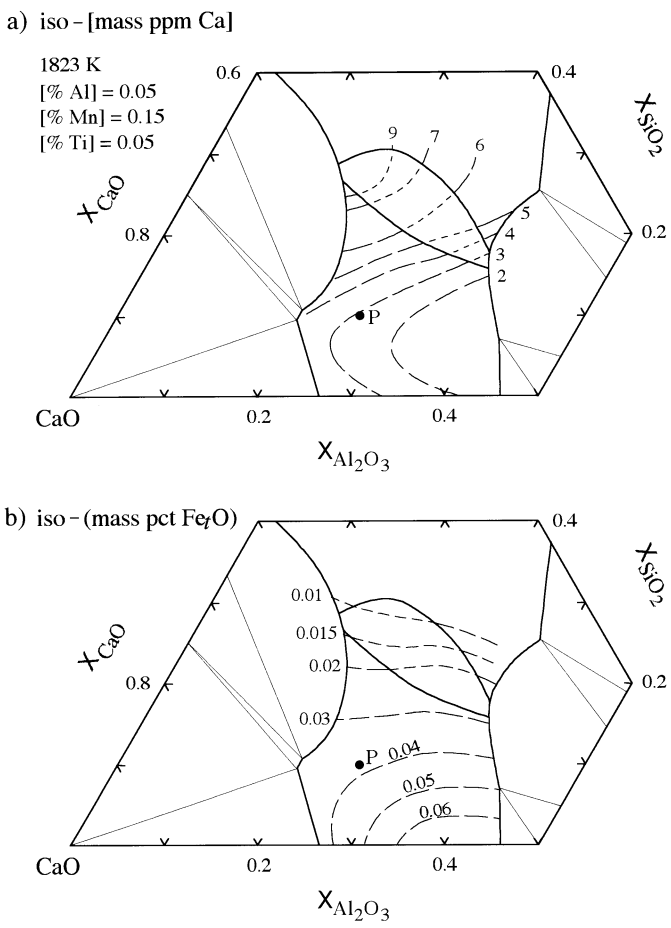

Fig. 14—(*a*) Iso-[mass ppm Ca] and (*b*) iso-(mass pct Fe_tO) lines at 1823 K for low carbon sheet steel.

which are used as one of the starting points in the Gibbs–Duhem integration, should be precisely determined experimentally. In addition to this, the modification of the present values of activities by using the thermochemical data on the interoxide compounds in this system is useful for a further check of the accuracy, if the accurate thermochemical data are available in the future.

REFERENCES

1. S. Maeda, T. Soejima, T. Saito, H. Matsumoto, H. Fujimoto, and T. Mimura: *Steelmaking Conf. Proc.*, 1989, pp. 379-85.
2. R.H. Rein and J. Chipman: *Trans. TMS-AIME*, 1965, vol. 233, pp. 415-25.
3. R. Schuhmann: *Acta Metall.*, 1955, vol. 3, pp. 219-26.
4. D.A.R. Kay and J. Taylor: *Trans. Faraday Soc.*, 1960, vol. 56, pp. 1372-83.
5. B. Ozturk and R.J. Fruehan: *Metall. Trans. B*, 1987, vol. 18B, pp. 746-49.
6. M.R. Kalyanram, T.G. Macfarlane, and H.B. Bell: *J. Iron Steel Inst.*, 1960, vol. 195, pp. 58-64.
7. F. Tamura and H. Suito: *Metall. Trans. B*, 1993, vol. 24B, pp. 121-30.
8. R. Inoue and H. Suito: *Metall. Trans. B*, 1992, vol. 23B, pp. 613-21.
9. S.-W. Cho and H. Suito: *Iron Steel Inst. Jpn. Int.*, 1994, vol. 34, pp. 177-85.
10. K.R. Lee and H. Suito: *Metall. Mater. Trans. B*, 1994, vol. 25B, pp. 893-902.
11. K. Tomioka and H. Suito: *Steel Res.*, 1992, vol. 63, pp. 1-6.
12. S.-W. Cho and H. Suito: *Iron Steel Inst. Jpn. Int.*, 1994, vol. 34, pp. 265-69.
13. H. Suito: *Proc. Ethem T. Turkdogan Symp. on Fundamentals and Analysis of New and Emerging Steelmaking Technologies*, Iron and Steel Society, TMS-AIME, and U.S. Steel Group of USX Corporation, Pittsburgh, PA, 1994, pp. 141-52.
14. H. Ohta and H. Suito: *Metall. Mater. Trans. B*, 1995, vol. 26B, pp. 295-303.
15. G.K. Sigworth and J.F. Elliott: *Met. Sci.*, 1974, vol. 8, pp. 298-310.
16. D.L. Sponseller and R.A. Flinn: *Trans. TMS-AIME*, 1964, vol. 230, pp. 876-88.
17. G. Yuancahng and W. Changzhen: *Metall. Trans. B*, 1990, vol. 21B, pp. 543-47.
18. G.G. Mikhailov and A.G. Tyurin: *Izv. Akad. Nauk SSSR, Metally*, 1984, No. 4, pp. 10-15.
19. *Recommended Values of Equilibrium Constants for the Reactions in Steelmaking*, Japan Society for the Promotion of Science, 19th Committee, Tokyo, 1984.
20. E.M. Levin, C.R. Robbins, and H.F. McMurdie: *Phase Diagram for Ceramists*, The American Ceramic Society, Columbus, OH, 1964, p. 219.
21. H. Sakai and H. Suito: *Iron Steel Inst. Jpn. Int.*, 1996, vol. 36, pp. 138-42.
22. J.F. Elliott, M. Gleiser, and V. Ramakrishna: *Thermochemistry for Steelmaking*, Addison-Wesley Publishing Co., Reading, MA, 1963, vol. 2.
23. E.T. Turkdogan: *Physical Chemistry of High Temperature Technology*, Academic Press, New York, NY, 1980, p. 8.
24. H. Gaye, C. Gatellier, M. Nadif, P.V. Riboud, J. Saleil, and M. Faral: *Rev. Metall.-CIT*, 1987, Nov., pp. 759-71.
25. M.W. Chase, Jr., C.A. Davies, J.R. Downey, Jr., D.J. Frurip, R.A. McDonald, and A.N. Syverud: *J. Phys. Chem. Ref. Data*, 1985, vol. 14, suppl. I (*JANAF Thermochemical Tables*).
26. H. Suito and R. Inoue: *Trans. Iron Steel Inst. Jpn.*, 1984, vol. 24, pp. 301-07.